

Supporting Information

Revealing the Electronic Structure of Silicon Intercalated Armchair Graphene Nanoribbons by Scanning Tunneling Spectroscopy

Okan Deniz¹, Carlos Sánchez-Sánchez^{1†}, Tim Dumsclaff², Xinliang Feng³, Akimitsu Narita², Klaus Müllen², Neerav Kharche⁴, Vincent Meunier⁴, Roman Fasel^{1, 5} and Pascal Ruffieux^{1}*

¹ Empa, Swiss Federal Laboratories for Materials Science and Technology, Überlandstrasse 129, CH-8600 Dübendorf, Switzerland

² Max Planck Institute for Polymer Research, Ackermannweg 10, D-55128 Mainz, Germany

³ Chair of Molecular Functional Materials, Department of Chemistry and Food Chemistry, Technische Universität Dresden, Mommsenstrasse 4, D-01062 Dresden, Germany

⁴ Department of Physics, Applied Physics, and Astronomy, Rensselaer Polytechnic Institute, Troy, New York 12180, United States

⁵ Department of Chemistry and Biochemistry, University of Bern, Freiestrasse 3, CH-3012 Bern, Switzerland

[†] Currently at Instituto de Ciencia de Materiales de Madrid (ICMM-CSIC), Sor Juana Inés de la Cruz 3, 28049 Madrid, Spain

Calibration of AuSIL coverage by STM

Prior to the intercalation experiments, we have calibrated the AuSIL coverage by STM. We have carried out different deposition experiments on Au(111) held at 475 K by only varying the Si deposition time. We show an STM image of a sub-ML AuSIL coverage sample in Figure S1. Here, we observe that Si adsorbed on the Au(111) surface transforms the herringbone reconstruction by nucleating possibly at the elbows of the herringbone reconstruction (Figure 1c) where a Au atom is missing. With increasing Si coverage, these nucleation areas laterally increase in size, then coalesce and eventually form extended islands, as is seen in Figure S1.

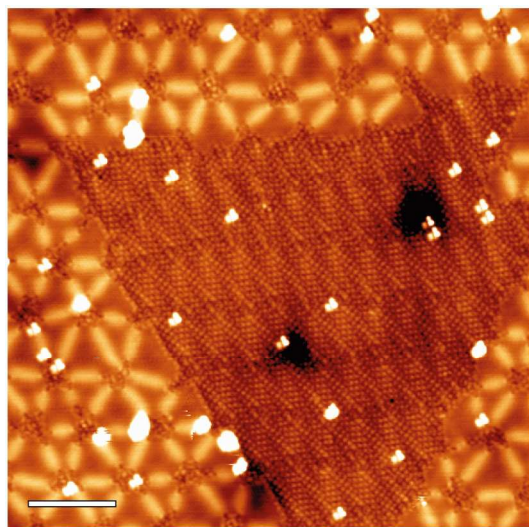


Figure S1. STM image of a sample exhibiting less than ML coverage of the AuSIL. Scale bar: 10 nm, $U = -1.5$ V, $I = 50$ pA

STM images of Si intercalated 21-AGNR

The corrugation of the AuSIL surface is visible through the GNRs in STM. Here, we show an example of an AuSIL-supported 21-AGNR segment. By differentiating the raw data shown in panel (a) it becomes evident that the corrugation visible on the GNR is similar to the one of the AuSIL substrate visible in the left part of the panel. Furthermore, the corrugation stemming from the armchair edge of the 21-AGNR is enhanced.

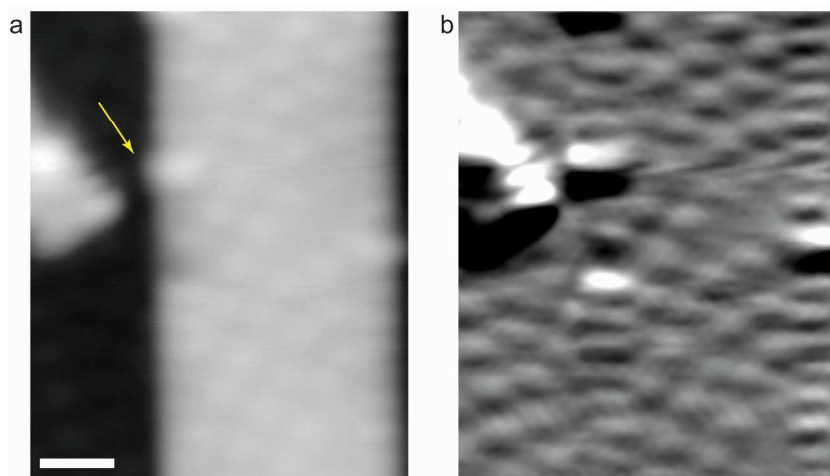


Figure S2. STM image of Si intercalated 21-AGNR: (a) unmodified STM topography image (the yellow arrow indicates an adsorbed Si adatom) and (b) vertically differentiated data of the STM image shown in (a). Scale bar: 1 nm, $U = -0.6$ V, $I = 400$ pA

Suppression of Au(111) surface state through AuSIL formation

We observe that surface alloying of Au results in the suppression of Au(111) state. To corroborate the disappearance of Au surface state, we prepare a sample with 7-AGNRs and we deposit Si with the same conditions reported in methods section, however at sub-ML regime so that the Au surface is only partially alloyed with Si. In this configuration it is possible to find 7-AGNRs adsorbed on either pure Au(111) or AuSIL. In Figure S3 below, we show two GNR segments on Au(111) and AuSIL.

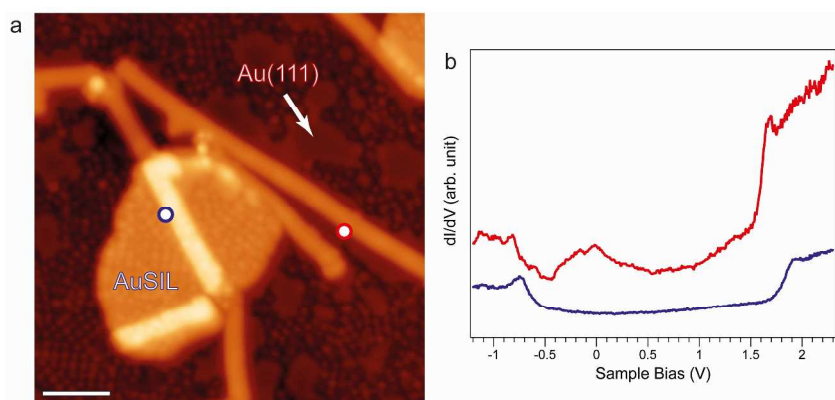


Figure S3. Sub-ML Si intercalated 7-AGNR on Au(111). (a) STM image shows the partial AuSIL formation below 7-AGNRs (Scale bar: 5 nm, $U = 1.5$ V, $I = 100$ pA) and (b) dI/dV spectra ($U = -0.8$ V, $I = 250$ pA) of two different 7-AGNR recorded on the positions marked by corresponding dot color in panel (a).

The STM image presented in panel (a) shows coexistence of Au(111) and AuSIL-adsorbed 7-AGNRs on this partially AuSIL-covered surface. While the remaining Au(111) domains appear as featureless areas in the STM image, the AuSIL domains reveal the same characteristic structure and corrugation as observed for the full monolayer AuSIL surface (see Figure 1d of the main text for comparison). In panel (b), the corresponding spectra from 7-AGNR on Au(111)

and 7-AGNR on AuSIL are shown. The spectra are recorded with the same tip condition and current setpoint. While the spectrum recorded for 7-AGNR on Au(111) reveals considerable contributions from the surface state, they vanish in the spectrum recorded on the 7-AGNR on AuSIL.

Series of single point spectra on 7-AGNR/AuSIL

A series of dI/dV spectra has been recorded along the edge of an AuSIL-supported 7-AGNR in order to determine the variation of the energy of frontier states for different positions of the AuSIL structure and due to the presence of Si adsorbates. The spectrum at the bottom of panel (b) was taken just next to the adsorbate which we expect to be a Si adatom. The spectral features of 7-AGNR's however do not change in energy. Only the intensity of the dI/dV signal is reduced due to the Si-induced modification of the apparent shape and related enhanced tip height near the Si adsorption site. All the other spectra show that the energy position of the frontier states is constant within the experimental error.

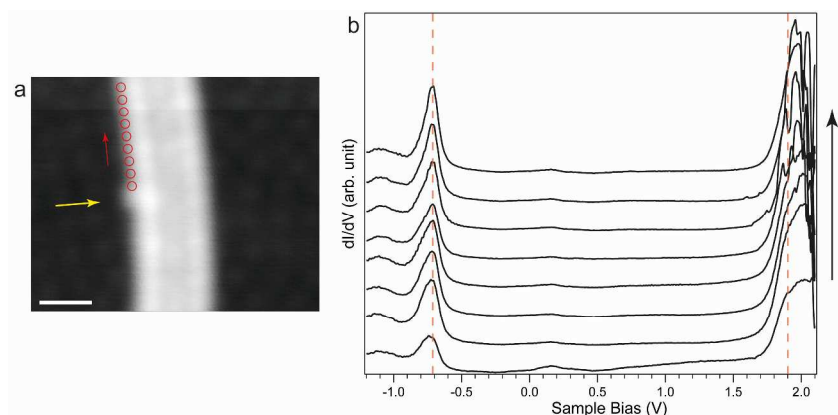


Figure S4. Series of spectra on 7-AGNR/AuSIL: (a) STM image of Si intercalated 7-AGNR.

The spectra have been taken on the red circles in the direction of the red arrow while the yellow arrow indicates the adsorbed Si adatom. (b) Series of spectra on 7-AGNR; the black arrow relates to the direction (red arrow in (a)) at which spectra have been taken. Scale bar: 1 nm, $U = -1.2$ V, $I = 1$ nA

dI/dV maps on 9-AGNR/AuSIL

Direct access to the spatial homogeneity of the frontier states of Si intercalated GNRs' is gained by recording dI/dV maps. While the topography images of GNRs on AuSIL systematically contain an apparent shape of the underlying AuSIL, the dI/dV maps are largely insensitive to the substrate and reveal a homogenous distribution of the frontier states. Their intensity is only lowered at positions where Si adatoms are adsorbed to the GNRs. Adsorbed Si, however, does not affect the energy position of the GNR states, as shown in Figure S4. It only affects the dI/dV intensity which we attribute to the increased apparent height of the GNR in the vicinity of adsorbed Si.

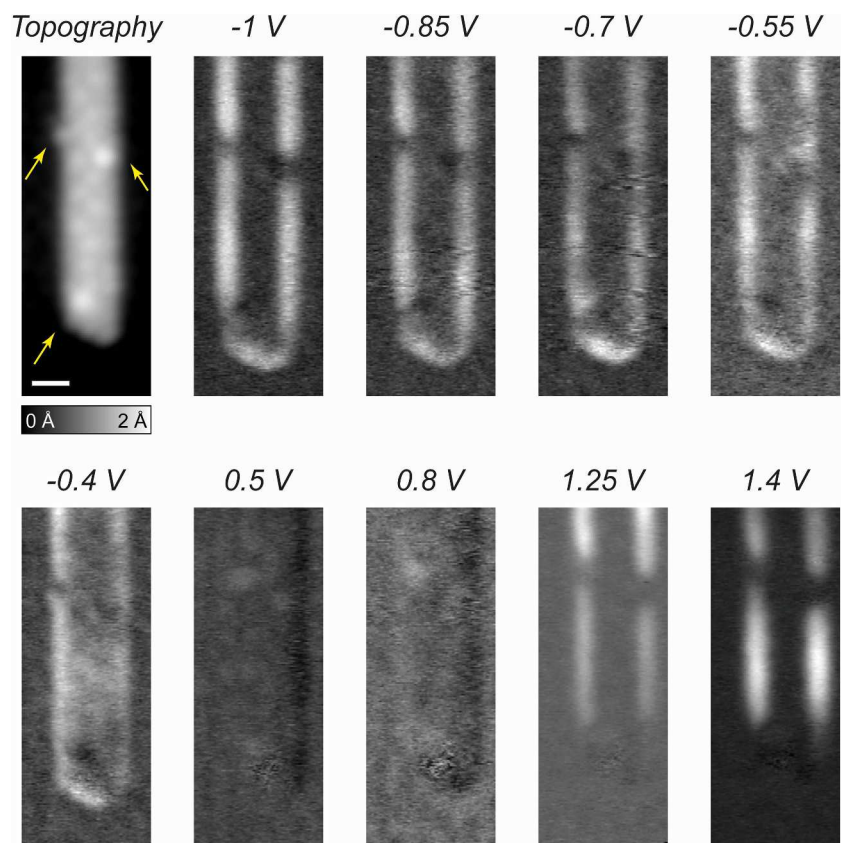


Figure S5. dI/dV maps recorded on 9-AGNR/AuSIL: Topography image: Scale bar: 1 nm, $U = 0.5$ V, $I = 150$ pA. Yellow arrows indicate the adsorbed Si adatoms. The dI/dV maps were recorded at constant current mode at 150 pA.

STM images of 7-, 9-, 14-, 18- and 21-AGNR segments

The wider derivatives of existing 7- and 9-AGNRs are fabricated by over-heating the samples to temperatures higher than the cyclodehydrogenation temperature of the GNRs. The dI/dV spectra shown in Figure 2e and Figure 3 of the main text are recorded on the corresponding segments below.

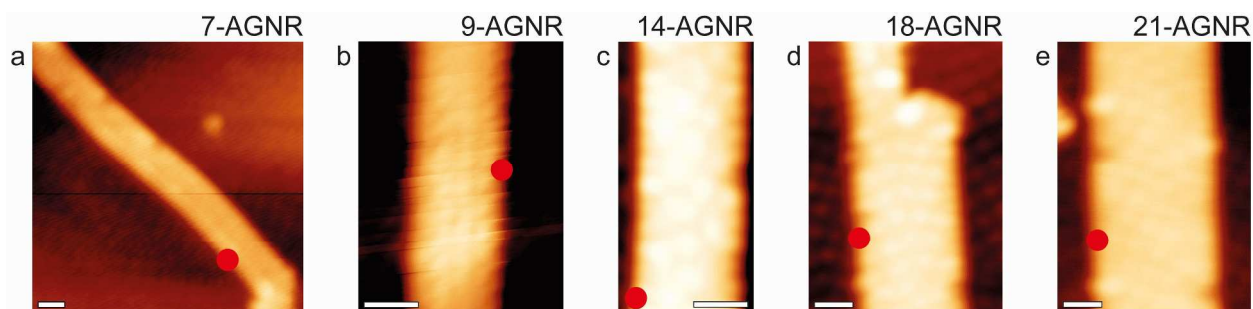


Figure S6. STM images of (a) 7-AGNR, (b) 9-AGNR, (c) 14-AGNR, (d) 18-AGNR and (e) 21-AGNR segments on AuSiL/Au(111). The scale bars are 1 nm. The red dots indicate the position where spectra shown in Figure 2e and Figure 3 have been recorded.

Calculated quasiparticle band gaps of AGNRs as a function of ribbon width together with the GW quasiparticle band gaps of isolated AGNRs

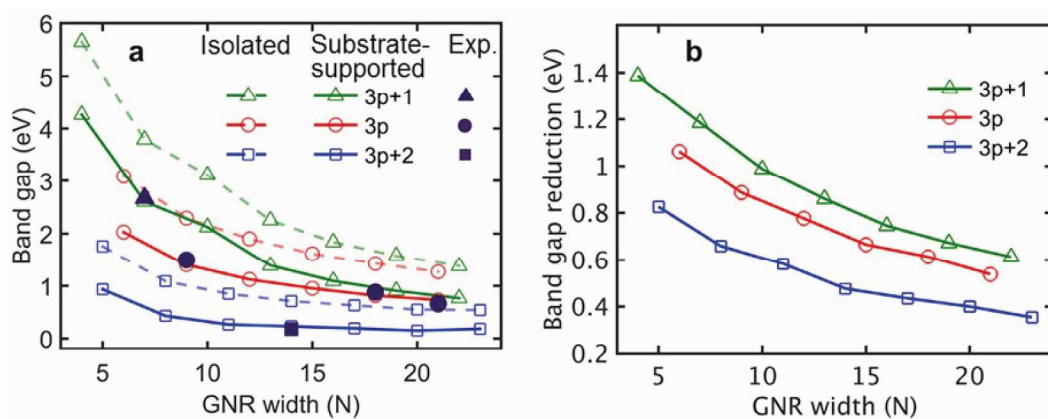


Figure S7. (a) Quasiparticle band gaps of isolated AGNRs and substrate-supported AGNRs as a function of ribbon width. The GW quasiparticle band gaps of isolated AGNRs, taken from Ref.,¹ are shown by the dashed lines. The full lines refer to the band gap values after correction for substrate screening within the advanced image-charge model.² (b) Substrate screening induced band gap reduction as a function of ribbon width.

The polarizability values of $3p$, $3p+1$ and $3p+2$ family AGNRs with respect to $1/E_g^2$

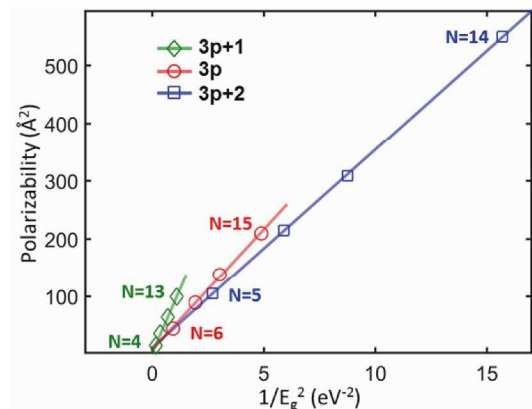


Figure S8. Polarizability (α) of AGNRs as a function of ribbon width calculated using the 1D Clausius–Mossotti expression $\alpha = (A/4\pi)(\varepsilon - 1)$, where A is the cross-section of the supercell and ε is the longitudinal dielectric constant, which is obtained using density functional perturbation theory (DFPT). Polarizability scales linearly as a function of $1/E_g^2$, where E_g is the DFT band gap. Carbon nanotubes have been shown to exhibit a similar scaling behavior.³ Due to the slow convergence of polarizability with respect to the supercell size, we use linear extrapolation to obtain polarizability of AGNRs with widths larger than $N = 15$.

REFERENCES

- (1) Zhu, X.; Su, H. *J. Phys. Chem. A* **2011**, *115* (43), 11998–12003.
- (2) Kharche, N.; Meunier, V. *J. Phys. Chem. Lett.* **2016**, *7* (8), 1526–1533.
- (3) Kozinsky, B.; Marzari, N. *Phys. Rev. Lett.* **2006**, *96* (16), 166801.